Time Domain Analysis of Grounding Electrodes Impulse Response

M. I. Lorentzou, N. D. Hatziargyriou, *Senior Member, IEEE*, and B. C. Papadias, *Life Fellow, IEEE*

***Abstract*—Lightning protection studies require estimation of grounding systems dynamic behavior. This paper presents the results of a new methodology for calculating the lightning response of the basic component of any grounding system, the grounding electrode. Lightning strike is modeled using a double exponential time function. Closed-form mathematical formulae are used to describe current and voltage distribution along the electrode. The effect of soil ionization can be also taken into account. The proposed methodology is validated by comparison of the obtained results with experimental and simulated waveforms found in literature.**

***Index Terms*—Grounding electrode, lightning protection, open-ended transmission line.**

I. Introduction

INCOMPLETE knowledge of the transient response of grounding electrodes results in almost empirical formulation of lightning protection methods [1]. Many attempts have therefore been made in the past for the calculation of this transient behavior. They can be divided in two main categories: 1) those based on frequency domain calculations with subsequent transformation of the solution in time domain using inverse fast Fourier transformation (IFFT); and 2) those based in calculation of the solution directly in the time domain.

Methods of the first category use an electromagnetic field approach for the calculation of the response of the grounding system in a wide range of frequencies [2], [3]. These methods, when applied in the analysis of fast transient phenomena, are characterized by increased accuracy because they are based strictly on the principles of electromagnetism and the least neglects possible are made. The fact that a system of equations has to be solved for every single frequency, however, increases significantly increases the computational time required.

Methods of the second category use a transmission line model of the electrode either trying to solve directly the telegraphy equations [4] and [5], or using a number of series connected π-circuits [6]–[8]. The latter is proved equivalent to a transmission line, when the number of circuits tends to infinite [9]. Most of these methods need to make low-frequency, quasistatic approximations. The upper frequency limit of satisfactory accuracy depends on the size of the electrode and the electrical characteristics of the surrounding soil [10]. Nevertheless, an error is introduced when phenomena involving high frequencies, such as lightning, are examined. An improved technique using J.Marti's approach for calculation of transients in transmission lines has been applied in [8], [11], [12]. Voltage and current values along the electrode are calculated using EMTP's frequency dependent transmission line model [13]. The main advantage of this method is the convenient incorporation of high frequencies making it suitable for lightning studies.

This paper presents a novel method for the analytical calculation of the behavior of a grounding electrode under transient conditions. The method belongs to the second category of methods (i.e., the grounding electrode is treated as an open-ended transmission line or as a series of π-circuits). Telegraphy equations are used and analytical formulae are obtained for current and voltage distributions along the electrode. The difference with previous attempts is that no particular assumptions for the energization source or the length of the electrode are required. For example, in [4] and [5], the electrode is assumed infinite, so that reflections at the far end can be neglected. Furthermore, in [4], a linearly increasing current at the start is considered and special assumptions for the Laplace inversion have been made. The algorithm described in [14] is based on prediction of the results from experimental data.

In the method proposed in the paper, lightning injection current is modeled as a typical double exponential function [15], although sinusoidal or other forms can be considered. Besides its generality, the method is characterized by accuracy, since it is based on closed form mathematical expressions. It is shown in the paper that from the infinite series of terms comprising the general solution for voltages and currents, only a small number of terms is needed to provide results of satisfactory accuracy in most practical cases. This remark leads to highly simplified solutions and allows very fast calculations with basic computing tools. Using this approach, results from the analytical calculation of the lightning response of horizontal grounding electrodes are presented. The impulse impedance, defined as the ratio of the instantaneous potential rise at the injection point to the energization current and the impulse coefficient, defined as the ratio of the impulse impedance to the power frequency resistance, are calculated. Finally, soil ionization phenomena are modeled considering a dynamic change of the radius of the grounding conductor. The results obtained are validated with experimental data and compared with results obtained from other analytical methods or numerical methods published in the literature [5], [7], [14], [16].

II. Theoretical Background

Grounding electrodes are characterized by per unit length series resistance R_e;, series inductance L_e; shunt conductance G_e;

Manuscript received May 15, 2000; revised May 13, 2002.

The authors are with the Electrical Engineering Department of NTUA, Athens, GR-15773, Greece (e-mail: lorentz@power.ece.ntua.gr; nh@power.ece.ntua.gr; papadias@power.ece.ntua.gr).

Digital Object Identifier 10.1109/TPWRD.2003.809686

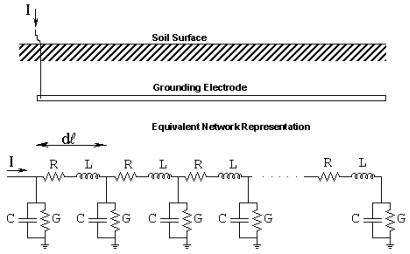

Fig. 1. Grounding electrode and its equivalent network representation.

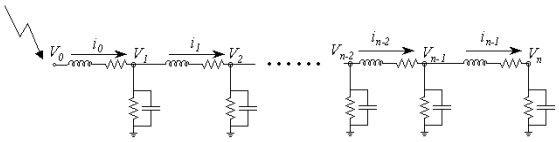

Fig. 2. Voltages and currents at lumped elements of the equivalent circuit network.

and shunt capacitance C_e. Voltage and current distribution along the electrodes must satisfy the telegraphy equations

$$-\frac{\partial V(x,t)}{\partial x} = R_e I(x,t) + L_e \frac{dI(x,t)}{dt}$$
$$-\frac{\partial I(x,t)}{\partial x} = G_e V(x,t) + C_e \frac{dV(x,t)}{dt}.$$

For the purposes of our analysis, grounding electrodes are modeled as a network of series connected π-equivalent circuits with lumped R–L–C elements, where each π-circuit corresponds to a small conductor segment (Fig. 1).

Mathematical analysis of this network requires

i) formulation of the expressions of voltages and currents for the equivalent network of π-circuits;
ii) calculation of their limits as the number of π-circuits increases.

For an infinite number of circuits, the network model of the electrode is equivalent to an open-ended transmission line [9]. Consequently, this procedure does not introduce any approximation.

The first stage of this calculation involves determination of the voltages and currents V_i, and i_i at each segment, as shown in Fig. 2.

For lightning studies, a source current of the form $i_0(t) = I_0 \cdot (e^{\alpha t} - e^{\beta t})$ is assumed. A linear differential equation with constant coefficients for the unknown voltage V_n at the end of the electrode as a function of the source current can be written as follows where $D = (d/dt)$, or

$$i_0 = (G + CD)(V_1 + V_2 + \cdots + V_n)$$
$$\Rightarrow \left.\begin{array}{c} i_0 = (G+CD)([(R+LD)i_1 + V_2] + V_2 + \cdots + V_n) \\ i_1 = (G+CD)(V_2 + V_3 + \cdots + V_n) \end{array}\right\} \Rightarrow$$

$$i_0 = B\left[(AB+2)V_2 + (AB+1)V_3 + \cdots + (AB+1)V_n\right] \quad (1)$$

where $A = R + LD$, $B = G + CD$.

Proceeding this way, a linear differential equation with constant coefficients involving only V_n and i_1 is obtained, as shown in the Appendix B(A.11).

A partial solution of this equation is

$$V_{n,p}(t) = \left(Cv_{\alpha,n}e^{\alpha\cdot t} - Cv_{\beta,n}e^{\beta\cdot t}\right) I_0$$

$C_{V_{\alpha,n}}, C_{v_{\beta,n}}$ are real constants. Going backward, it is

$$i_{n-1,p}(t) = (G+CD)V_{n,p}(t)$$
$$= \left\lfloor (G+aC)Cv_{\alpha,n}e^{\alpha t} - (G+\beta C)Cv_{\beta,n}e^{\beta t} \right\rfloor I_0.$$

Following a similar approach, a partial solution of the differential equation considering current at the k circuit, is of the form

$$\frac{i_k}{I_0} = C_{\alpha,k}e^{\alpha\cdot t} - C_{\beta,k}e^{\beta\cdot t} \quad (2)$$

where $C_{\alpha,k}C_{\beta,k}$ are constants.

The Kirchoff' s laws for voltages and currents need to be satisfied at any point of the network, providing (see Appendix A)

$$\lim_{n\to\infty} i_k(t) = I_p(x,t)$$
$$= I_0\left(\frac{\sinh\left(\gamma_\alpha(\ell - x)\right)}{\sinh\left(\gamma_\alpha \ell\right)}e^{\alpha\cdot t} - \frac{\sinh\left(\gamma_\beta(\ell - x)\right)}{\sinh\left(\gamma_\beta \ell\right)}e^{\beta\cdot t}\right). \quad (3)$$

Telegraphy equations result in voltage distribution as follows:

$$V_p(x,t) = I_0\left(\frac{-\cosh\left(\gamma_\alpha(\ell - x)\right)}{\sinh\left(\gamma_\alpha \ell\right)} \cdot \frac{\gamma_\alpha}{G_e + \alpha\cdot C_e}e^{\alpha\cdot t} - \frac{-\cosh\left(\gamma_\beta(\ell - x)\right)}{\sinh\left(\gamma_\beta \ell\right)} \cdot \frac{\gamma_\beta}{G_e + \beta\cdot C_e}e^{\beta\cdot t} + \text{const}\cdot e^{-(G_e t/C_e)}\right) \quad (4)$$

where $\gamma_\alpha = \sqrt{(R_e + \alpha L_e)(G_e + \alpha C_e)}$ and $\gamma_\beta = \sqrt{(R_e + \beta L_e)(G_e + \beta C_e)}$.

The above partial solution must be completed by the general solution of the homogeneous differential equation. This is expressed by the following equations for current and voltage, correspondingly (see Appendix B):

$$I_h(x,t) = I_0\sum_{k=1}^{\infty}\left\{C_1(k)\cdot\frac{\sinh\left(\gamma_{r_1(k)}(\ell - x)\right)}{Z_{r_1}(k)}\cdot e^{r_1(k)\cdot t} + C_2(k)\cdot\frac{\sinh\left(\gamma_{r_2(k)}(\ell - x)\right)}{Z_{r_2}(k)} \cdot e^{r_2(k)\cdot t}\right\} \quad (5)$$

$$V_h(x,t) = I_0\sum_{k=1}^{\infty}\left\{C_1(k)\cdot\cosh\left(\gamma_{r_1(k)}(\ell - x)\right)\cdot e^{r_1(k)\cdot t} + C_2(k)\cdot\cosh\left(\gamma_{r_2(k)}(\ell - x)\right) \cdot e^{r_2(k)\cdot t}\right\} \quad (6)$$

where

$$r_1(k) = \frac{-R_eC_e\ell^2 - L_eG_e\ell^2 + \Delta}{2L_eC_{+e}}$$
$$r_2(k) = \frac{-R_eC_e\ell^2 - L_eG_e\ell^2 - \Delta}{2L_eC_e}$$
$$\Delta = \sqrt{(R_eC_e\ell^2 - L_eG_e\ell^2)^2 - 4L_eC_e\ell^2 - \pi^2k^2}$$
$$Z_{r_1}(k) = \sqrt{\frac{R_e + r_1(k)L_e}{G_e + r_1(k)C_e}} \quad Z_{r_2}(k) = \sqrt{\frac{R_e + r_2(k)L_e}{G_e + r_2(k)C_e}}$$
$$\gamma_{r_i(k)} = \sqrt{(R_e + r_i(k)L_e)(G_e + r_i(k)C_e)}.$$

Consequently, current and voltage at any point of the electrode at any time are given by (7)

$$\begin{aligned} I(x,t) &= I_h(x,t) + I_p(x,t) \\ V(x,t) &= V_h(x,t) + V_p(x,t). \end{aligned} \tag{7}$$

Expressions (5) and (6) comprise sums of infinite terms, only a few terms are needed, however, to approximate the solution with satisfactory accuracy.

The number of these terms depends on the electrode length, soil resistivity, relative permittivity ε_r, and the rise time of the injection current. It increases as the length of the electrode increases and as the soil permittivity decreases. It should be noted that accuracy within less than 1% is obtained with only one term when the response of electrode lengths shorter than the "effective length" determined in [9], is calculated. In electrodes longer than the "effective length," however, three terms provide results with an error $<1\%$ in all practical cases examined. These terms should be selected from the values of $r_{1,2}(k)$ which are close to the parameters of the injected double exponential α, β.

The fact that very few terms are needed in the final expressions (5) and (6) greatly simplifies the method making it suitable for use in analytical calculations. It should be noted that apart from this simplification, closed form expressions have been used in the main stages of the procedure, ensuring results of high accuracy.

All constants $C_1(k)$ and $C_2(k)$ in (5) and (6) and *const* in (3) are determined in order to satisfy the initial conditions of propagation of current and voltage travelling waves

$$\begin{aligned} I\left(x, x\sqrt{L_eC_e}\right) &= 0 \\ V\left(x, x\sqrt{L_eC_e}\right) &= 0 \end{aligned} \tag{8}$$

or

$$I_h\left(x, x\sqrt{L_eC_e}\right) + I_p\left(x, x\sqrt{L_eC_e}\right) = 0 \tag{9}$$

$$V_h\left(x, x\sqrt{L_eC_e}\right) + V_p\left(x, x\sqrt{L_eC_e}\right) = 0. \tag{10}$$

It is convenient to use the auxiliary functions

$$\begin{aligned} f(k,x) &= \sum_{i=1,2} \frac{\sinh\left(\gamma_{r_i(k)}(\ell - x)\right)}{Z_{r_i}(k)} \cdot e^{r_i(k)\cdot x\cdot\sqrt{L_eC_e}} \\ g(k,x) &= \sum_{i=1,2} \cosh\left(\gamma_{r_i(k)}(\ell - x)\right) \cdot e^{r_i(k)\cdot x\cdot\sqrt{L_eC_e}} \\ g1(x) &= e^{-(G_e/C_e)\cdot x\cdot\sqrt{L_eC_e}} \end{aligned} \tag{11}$$

$C_1(k)$ are set equal to $C_2(k)$, in order to have real values of $I_h(x,t)$ and $V_h(x,t)$ when the roots $r_i(k)$ are complex, but this works well also when the roots are real. There are two possible ways to determine $C_i(k)$: using (9) or using (10). For example, using (10), the following equations are formed:

$$\begin{aligned} C_i(1\ldots k_{\max}-1) &= \underline{B}^{-1}\cdot\underline{V}_p(1\ldots k_{\max}-1) \\ \text{const} &= \underline{B}^{-1}\cdot\underline{V}_p(k_{\max}) \end{aligned} \tag{12}$$

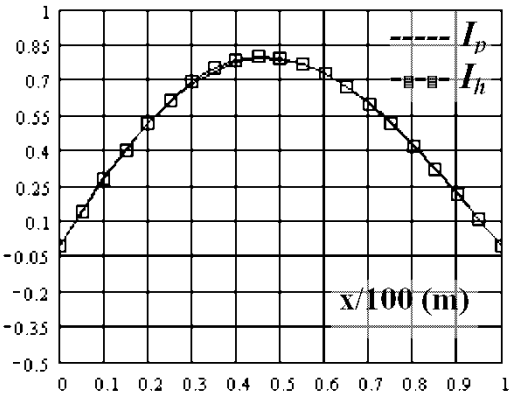

(a)

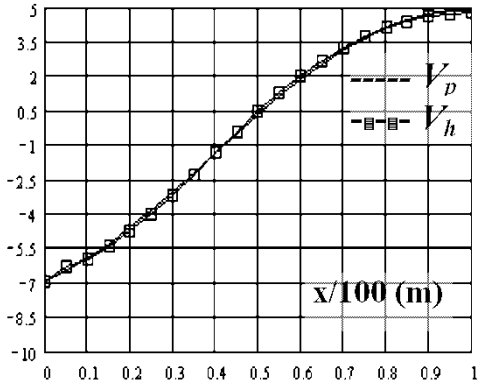

(b)

Fig. 3. (a) Comparison of $I_h(x, x\sqrt{L_eC_e})$ and $I_p(x, x\sqrt{L_eC_e})$. (b) Comparison of $V_h(x, x\sqrt{L_eC_e})$ and $V_p(x, x\sqrt{L_eC_e})$.

where

$$\begin{aligned} \underline{B}(i, 1\ldots k_{\max}-1) &= g\left(1\ldots k_{\max}-1, i\cdot\frac{\ell}{k_{\max}}\right) \\ \underline{B}(i, k_{\max}) &= g1\left(i\cdot\frac{\ell}{k_{\max}}\right) \\ \underline{V}_p(k) &= V_p\left(k\cdot\frac{\ell}{k_{\max}}, k\cdot\frac{\ell}{k_{\max}}\cdot\sqrt{L_eC_e}\right). \end{aligned}$$

Almost accurate match is achieved between $I_h(x, x\sqrt{L_eC_e})$ and $I_p(x, x\sqrt{L_eC_e})$ and between $V_h(x, x\sqrt{L_eC_e})$ and $V_p(x, x\sqrt{L_eC_E})$ as shown in Fig. 3 for the case of a 100-m-long electrode in 100-Ωm soil with $\varepsilon_r = 4$ excited by a 8/20-μs current. Coefficients $C_I(k)$ are $C(1) = 5.771$, $C(2) = -0.589$, const $= 5.858$.

A. Analysis of Travelling Waves

In the expressions (3)–(6), forward and backward travelling waves can be distinguished for current

$$\begin{aligned} I^{\pm}(x,t) = &\frac{\pm e^{\alpha\cdot t\pm\gamma_\alpha(\ell-x)}}{\sinh(\gamma_\alpha\ell)} - \frac{\pm e^{\beta\cdot t\pm\gamma_\beta(\ell-x)}}{\sinh(\gamma_\beta\ell)} \\ &\mp\sum_{k=1}^{\infty}\left\{C_1(k)\cdot\frac{e^{r_1(k)\cdot t\pm\gamma_{r_1(k)}(\ell-x)}}{Z_{r_1}(k)}\right. \\ &\left.+C_2(k)\cdot\frac{e^{r_2(k)\cdot t\pm\gamma_{r_2(k)}(\ell-x)}}{Z_{r_2}(k)}\right\} \end{aligned} \tag{13}$$

TABLE I
INPUT DATA FOR MODEL APPLICATION

Test electrode	Injection Current
Length = 100m Diameter = 3mm Burial depth = 0.60m	$I_{source}(t) = I_0 \cdot (e^{\alpha t} - e^{\beta t})$ I_0 = 1.55227 A
ρ_e =0.25 E-6 Ohm-m	α = -3640, β = -652210

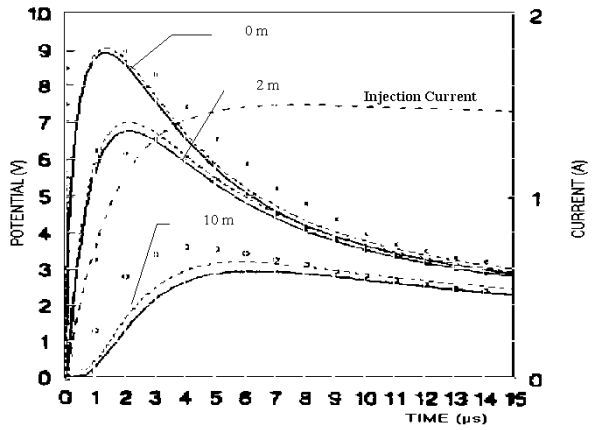

Fig. 4. Response under an impulse strike from (a) —EMTP. (b) - - - - Analytical formulae (7). (c) o o o experimental data.

and for voltage

$$V^{\pm}(x,t) = \frac{-e^{a\cdot t \pm \gamma_\alpha(\ell - x)}}{\sinh(\gamma_\alpha \ell)} \cdot \frac{\gamma_\alpha}{G_e + \alpha C_e} - \frac{-e^{\beta\cdot t \pm \gamma_\beta(\ell - x)}}{\sinh(\gamma_\beta \ell)} \cdot \frac{\gamma_B}{G_e + \beta C_e} - \sum_{k=1}^{\infty} \left\{ C_1(k) \cdot e^{r_1(k)\cdot t \pm \gamma_{r_1(k)}(\ell - x)} + C_2(k) \cdot e^{r_2(k)\cdot t \pm \gamma_{r_2(k)}(\ell - x)} \right\} \quad (14)$$

In (13), $I^+(x,t)$ is the sum of all forward current waves, and $I^-(x,t)$ is the sum of all backward waves. Total current at point is given as the sum $I(x,t) = I^+(x,t) + I^-(x,t)$. A similar expression is used for voltage $V(x,t) = V^+(x,t) + V^-(x,t)$.

III. MODEL VALIDATION

Validation of the proposed method is based on experimental data from literature [7]. Test electrode and injection current are described in Table I. Soil has resistivity 20 Ωm and permittivity 80. Current injected has low values so soil ionization phenomena can be neglected.

Results are plotted in the following Fig. 4. They are contrasted to experimental data and results obtained from EMTP, where the electrode is modeled using a series of pi-circuits, similar to the model of Fig. 1. It is shown that the results are almost identical to those from EMTP and close to experimental ones.

IV. APPLICATION

The proposed model is applied to the transient analysis of a 140-m-long electrode with a radius of 1.5 mm, buried in 0.9 m in 300 Ω m soil. Injection current has a 7/28-μs waveform. Current

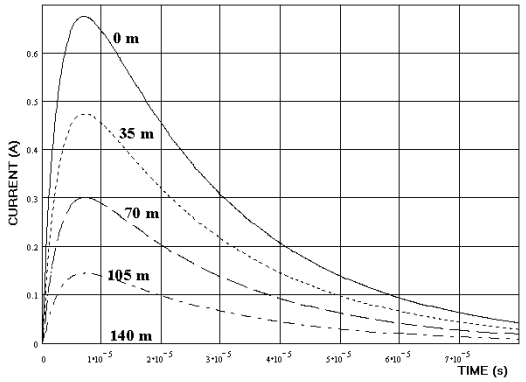

Fig. 5. Current distribution versus time at various points of a 140-m-long electrode buried in high relative permittivity soil ($\varepsilon_r = 50$).

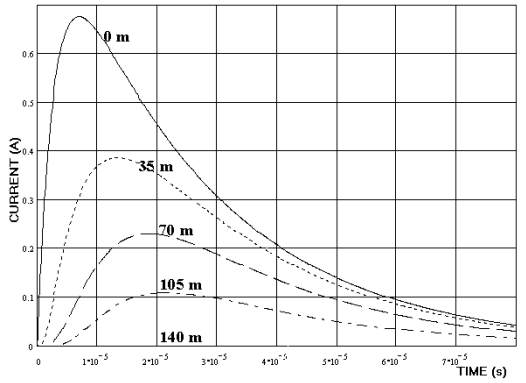

Fig. 6. Current distribution versus time at various points of a 140-m-long electrode buried in low relative permittivity soil ($\varepsilon_r = 1$).

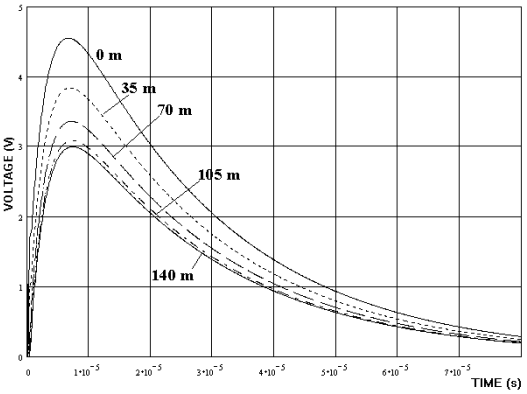

Fig. 7. Voltage distribution versus time at various points of a 140-m-long electrode buried in high relative permittivity soil ($\varepsilon_r = 50$).

and voltage values at various points of the electrode are shown in Figs. 5–8.

It can be observed that currents and voltages at any point of the electrode have almost the same waveshape versus time as the injected current when $\varepsilon_r = 50$ (Figs. 5 and 7). When relative permittivity is low, the effect of the capacitive component weakens. In this case, the electrode shows a reactive behavior. This results in faster appearance of the voltage peak (Fig. 8) at the injection point and distortion of the current waveshape along the electrode (Fig. 6).

Maximum current value decreases as the distance from the start increases, until it reaches zero at the electrode end. This is

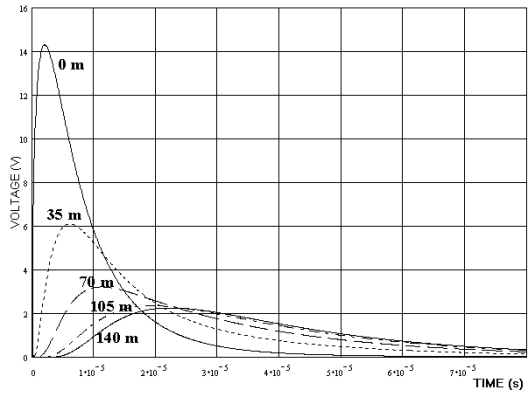

Fig. 8. Voltage distribution versus time at various points of a 140-m-long electrode buried in low relative permittivity soil $(\varepsilon_r = 1)$.

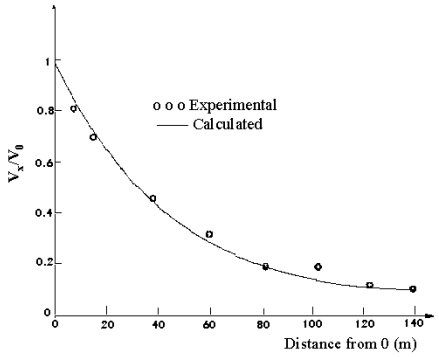

Fig. 9. V_x/V_o ratio versus electrode length (m).

expected from the theory of travelling waves at the open-ended transmission line, since current waves are fully reflected at the end of the electrode, giving a zero total current value at this point.

The ratio of the maximum voltage at any fixed distance x to the maximum voltage at the current injection point decreases as the electrode length increases, because the increased length weakens the effect of superposition of reflections at the end. This is shown in Fig. 9 where experimental results [5] and analytical formulae (7) have been contrasted for the calculation of V_x/V_0 ratio for the simulated 140-m-long electrode in 300 Ω m soil.

Impulse impedance is defined as the ratio of the transient potential at the injection point to the current injected

$$Z(0,t) = \frac{V(0,t)}{I(0,t)}.$$

In general, it has higher values than the steady state resistance, although a lower value may appear at the first ìs depending on the electrode characteristics. An example of impulse impedance calculation can be seen in Fig. 10, where calculation results for 30.48-m-long electrode buried in various soils appear to agree well with experimental data [14].

V. Soil Ionization

When large current densities are injected in the electrode, large currents emanate from its surface to the soil. When the critical field strength exceeds a particular value, breakdown of

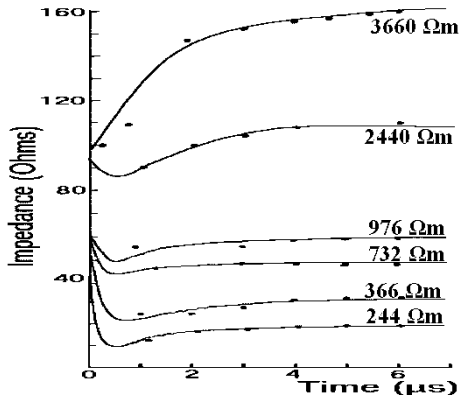

Fig. 10. Impulse impedance from (a) ••• Experimental data. (b) — Analytical formulae.

the soil occurs. In this case, the electrode will be surrounded by a cylindrical corona-type discharge pattern, which augments its practical radius and makes the dispersion of the current from its surface to the earth easier. The critical breakdown strength E_{crit} of the surrounding soil can be obtained from the following formula [17]:

$$E_{\text{crit}} = 241 \cdot \sigma_E^{-0.215} \tag{15}$$

where E_{crit} is in kilovolts per meter and σ_E is in $(\Omega\text{m})^{-1}$.

According to [16], soil resistivity of the surrounding soil decays in an exponential manner, when ionization occurs. At the deionization phase, it recovers also in an exponential way. In the method proposed in this paper, soil ionization can be easily accommodated at a given time t by modification of the electrode radius as follows.

1) Current and voltage distribution along the electrode are calculated for given soil characteristics, impulse current, and electrode geometry.
2) The field strength is calculated, leading to a respective change of the conductor radius, if applicable. Modified conductor radius is given from the formula $r = (I\rho/2\pi l E_c)$ where I is the leakage current at a discrete point, ρ is the resistivity of soil, and E_c is the critical electric field intensity value.
3) Current and voltage distributions are calculated for the new radius of the conductor which is changing along the electrode. This results in modification of R–L–C parameters of the equivalent ladder network that represents the electrode, according to an exponential rule. The rest of injection current is considered as energization source. Current and voltage values at time t form the initial conditions for the calculation of current and voltage distributions at the next time steps.
4) For the next time, steps 2 and 3 are repeated.

Using the proposed method, the experimental results presented in [18] are reproduced.

The electrode under consideration is a 8.61-m buried horizontal electrode excited by 22.2-kA impulse current. Voltages and currents have been calculated for the first 30 μs. Raised potential at the injection point of the electrode has been calculated for injection of 15 kA and it is contrasted to experimental values in Fig. 11.

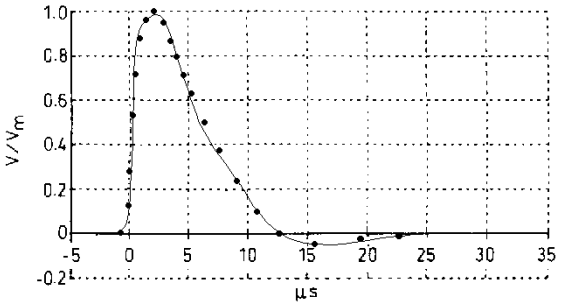

Fig. 11. Voltages produced at ionized electrode (a) ___ Calculated. (b) • • • Experimental (22.2 kA).

VI. Conclusions

In this paper, a new method for the analysis of the transient behavior of grounding electrodes is presented. It is characterized by the following advantages.

- The method is based on closed form solution of the telegraphy equations. The solution is achieved directly in time domain, so any transformation to and from the frequency domain is not required.
- The method is general (i.e., no particular assumptions for the form of the energization source or the length of the electrode are required).
- Convergence to fifth decimal point is achieved using only a few terms (up to four) of the infinite series expressing analytically the current and voltage distributions, while the initial conditions are fully satisfied. This simplification simplifies and accelerates calculations.
- Results compare very satisfactorily with field measurements or results from other analytical or numerical methods. A good agreement is also observed in case soil ionization is incorporated in the analysis.

Appendix A
Formulation of Partial Solution for Current and Voltage Along the Electrode

Kirchoff's currents law at node k of the circuit in Fig. 12 is written

$$i_k - i_{k+1} = GV_{k+1} + C\frac{dV_{k+1}}{dt}. \tag{A.1}$$

Considering a current distribution of the form described in (2), integration of (A.1) gives

$$V_{k+1} = \frac{C_{\alpha,k} - C_{\alpha,k+1}}{G+\alpha\cdot C}e^{\alpha\cdot t} - \frac{C_{\beta,k} - C_{\beta,k+1}}{G+\beta\cdot C}e^{\beta\cdot t} + \text{const}\cdot e^{-(Gt/C)}. \tag{A.2}$$

Kirchoff's law for voltages at the k-th circuit is written

$$V_{k+1} = V_{k+2} + Ri_{k+1} + L\frac{di_{k+1}}{dt}. \tag{A.3}$$

Replacing in (A.3), V_{k+1} and V_{k+2} from (A.2) and i_{k+1} from (2), we obtain from (A.3)

$$\begin{aligned} C_{\alpha,k} &= [2+(R+\alpha L)(G+\alpha C)]\,C_{\alpha,k+1} - C_{\alpha,k+2} \\ C_{\beta,k} &= [2+(R+\beta L)(G+\beta C)]\,C_{\beta,k+1} - C_{\beta,k+2}. \end{aligned} \tag{A.4}$$

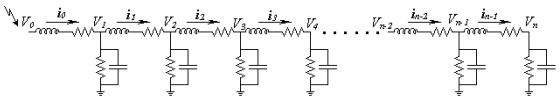

Fig. 12. Voltages and current at lumped elements of the equivalent circuit network

The relations (A.4) shown before take a different form at the start of the electrode

$$\begin{aligned} 1 &= [2+(R+\alpha L)(G+\alpha C)]\,C_{\alpha,1} - C_{\alpha,2} \\ 1 &= [2+(R+\beta L)(G+\beta C)]\,C_{\beta,1} - C_{\beta,2} \end{aligned} \tag{A.5}$$

and at the end of the electrode

$$\begin{aligned} C_{\alpha,n-2} &= [2+(R+\alpha L)(G+\alpha C)]\,C_{\alpha,n-1} \\ C_{\beta,n-2} &= [2+(R+\beta L)(G+\beta C)]\,C_{\beta,n-1}. \end{aligned} \tag{A.6}$$

Coefficients $C_{\alpha,k}$ and $C_{\beta,k}$ that fully satisfy (A.4)–(A.6) are given as

$$C_{\alpha,k} = \frac{\alpha_1^{k-2}\left(\beta_1^{2n-4}-1\right) + \beta_1^{k-2}\left(\alpha_1^{2n-4}-1\right)}{\beta_1^2\left(\beta_1^{2n-4}-1\right) + \alpha_1^2\left(\alpha_1^{2n-4}-1\right)} \tag{A.7}$$

where

$$\begin{aligned} \alpha_1 &= \frac{p+\sqrt{p^2-4}}{2} \\ \beta_1 &= p-\alpha_1 \\ p &= 2+(R+\alpha L)(G+\alpha C). \end{aligned}$$

The limit of (A.7) as the number n of segments tends to infinity, is calculated as follows.

Increasing the number of segments a point of the electrode in $x(m)$ from the start, corresponds to k circuit with $k = nx/\ell$. Consequently, it is

$$\begin{aligned} &\lim_{n\to\infty} C_{\alpha,k} \\ &= \lim_{n\to\infty} \frac{\alpha_1^{k-2}\left(\beta_1^{2n-4}-1\right) + \beta_1^{k-2}\left(\alpha_1^{2n-4}-1\right)}{\beta_1^2\left(\beta_1^{2n-4}-1\right) + \alpha_1^2\left(\alpha_1^{2n-4}-1\right)} \\ &= \lim_{n\to\infty} \frac{\alpha_1^{(nx/\ell)-2}\left(\beta_1^{2n-4}-1\right) + \beta_1^{(nx/\ell)-2}\left(\alpha_1^{2n-4}-1\right)}{\beta_1^2\left(\beta_1^{2n-4}-1\right) + \alpha_1^2\left(\alpha_1^{2n-4}-1\right)} \end{aligned}$$

It is $\lim_{n\to\infty}\alpha_1 = \lim_{n\to\infty}(p+\sqrt{p^2-4})/2$ where

$$\lim_{n\to\infty} p = \lim_{n\to\infty}\left[2+\left(\frac{R_e\ell}{n}+\alpha\frac{L_e\ell}{n}\right)\left(\frac{G_e\ell}{n}+\alpha\frac{C_e\ell}{n}\right)\right] = 2. \tag{A.8}$$

So $\lim_{n\to\infty}\alpha_1 = 1$ and $\lim_{n\to\infty}\beta_1 = \lim_{n\to\infty}(p-\alpha_1) = 2-1=1$

$$\lim_{n\to\infty}\alpha_1^n = \lim_{n\to\infty}\left[1+\frac{(R_e+aL_e)(G_e+aC_e)\ell^2}{2n^2} + \sqrt{\left(1+\frac{(R_e+aL_e)(G_e+aC_e)\ell^2}{2n^2}\right)^2-1}\right] = e^{\gamma a\ell}$$

where $\gamma_\alpha = \sqrt{(R_e + \alpha L_e)(G_e + \alpha C_e)}$

$$\lim_{n\to\infty} \beta_1^n = \lim_{n\to\infty} \left(\frac{1}{\alpha_1}\right)^n = e^{-\gamma_\alpha \ell}.$$

Limit of $C_{\alpha,k}$ is finally

$$\begin{aligned}\lim_{n\to\infty} C_{\alpha,k} =& \frac{e^{\gamma_\alpha x}\left(e^{-2\gamma_\alpha \ell}-1\right) + e^{-\gamma_\alpha x}\left(e^{2\gamma_\alpha \ell}-1\right)}{\left(e^{-2\gamma_\alpha \ell}-1\right)+\left(e^{2\gamma_\alpha \ell}-1\right)} \\ =& \frac{\cosh\left(\gamma_\alpha\left(x-2\ell\right)\right)-\cosh\left(\gamma_\alpha x\right)}{\cosh\left(2\gamma_\alpha \ell\right)-1} \\ =& \frac{\sinh\left(\gamma_\alpha\left(\ell-x\right)\right)}{\sinh\left(\gamma_\alpha \ell\right)}. \end{aligned} \tag{A.9}$$

Placing $C_{\alpha,k}$ as given from (A.9) and a similar expression for $C_{\beta,k}$ in relation (2), we obtain (3).

Appendix B
Formulation of Solution of Homogeneous Equations for Current and Voltage Along the Electrode

From Fig. 12, we obtain

$$i_0 = GV_1 + C\frac{dV_1}{dt} + i_1. \tag{A.10}$$

We set $D = d/dt$, $A = R + LD$, $B = G + CD$.

Going backward from the end of the electrode to the start, it can be proved by induction that it is

$$i_0 = \frac{\alpha_2^2\left(-\frac{\alpha_2}{\beta_2}\right)^{n-1} - \beta_2^2\left(-\frac{\beta_2}{\alpha_2}\right)^{n-1}}{\beta_2 - \alpha_2} V_n \tag{A.11}$$

where$\alpha_2 = \left[-AB + \sqrt{AB\left(AB+4\right)}\right]/2A$ and $\beta_2 = -B - \alpha_2$.

Expansion of the second part of (A.11) is a linear differential equation of V_n with constant coefficients, of order $n+2$. Corresponding homogeneous (A.12) has a general solution, which is expressed as a linear combination of exponentials, one for each simple root of the characteristic polynomial

$$\frac{\alpha_2^2\left(-\frac{\alpha_2}{\beta_2}\right)^{n-1} - \beta_2^2\left(-\frac{\beta_2}{\alpha_2}\right)^{n-1}}{\beta_2 - \alpha_2} V_n = 0. \tag{A.12}$$

In this case, roots of the characteristic polynomial are simple. Determination of roots has been done only after calculation of $\lim_{n\to\infty}(\alpha_2^2\left(-\alpha_2/\beta_2\right)^{n-1} - \beta_2^2\left(-\beta_2/\alpha_2\right)^{n-1}/\beta_2 - \alpha_2)$, which is found following a similar procedure to the one described in (A.1). It is

$$\begin{aligned}\lim_{n\to\infty} & \frac{\alpha_2^2\left(-\frac{\alpha_2}{\beta_2}\right)^{n-1} - \beta_2^2\left(-\frac{\beta_2}{\alpha_2}\right)^{n-1}}{\beta_2 - \alpha_2} \\ & = -\sqrt{\left(\frac{G_e + xC_e}{R_e + xL_e}\right)} \cdot \sinh(\gamma_x \ell). \end{aligned} \tag{A.13}$$

Solutions of (A.13) are $x = -(G_e/C_e)$ and

$$\begin{aligned}\gamma_r \ell =& k\pi j, \quad k = \pm 1, 2, 3 \ldots \infty \Rightarrow \\ r_1(k) =& \frac{1}{2L_eC_e} \\ & \cdot \Big(-R_eC_e\ell^2 - L_eG_e\ell^2 \\ & \quad + \sqrt{\left(R_eC_e\ell^2 - L_eG_e\ell^2\right)^2 - 4L_eC_e\ell^2\pi^2k^2}\Big) \\ r_2(k) =& \frac{1}{2L_eC_e} \\ & \cdot \Big(-R_eC_e\ell^2 - L_eG_e\ell^2 \\ & \quad - \sqrt{\left(R_eC_e\ell^2 - L_eG_e\ell^2\right)^2 - 4L_eC_e\ell^2\pi^2k^2}\Big). \end{aligned}$$

Consequently, the general solution of the homogeneous equation for the voltage at the end is written

$$V_h(x,t) = \sum_{k=1}^{\infty}\left\{C_1(k)\cdot e^{r_1(k)\cdot t} + C_2(k)\cdot e^{r_2(k)\cdot t}\right\}. \tag{A.14}$$

Going backward in the circuit of Fig. 12 at a point k segments from the start, it is

$$i_{k-1} = \frac{\alpha_2^2\left(-\frac{\alpha_2}{\beta_2}\right)^{n-k} - \beta_2^2\left(-\frac{\beta_2}{\alpha_2}\right)^{n-k}}{\beta_2 - \alpha_2} V_n \tag{A.15}$$

where α_2 and β_2 are as in (A.11). Calculation of the limit of (A.15) as n tends to infinity, and use of (A.14) leads to expression (5). Use of the telegraphy equations leads to expression (6) for voltage distribution along the electrode.

References

[1] *Protection of Structures Against Lightning, Part 1: General Principles*, IEC 1024-1-1:1993, 1993.

[2] L. Grcev and V. Arnautovski, "Frequency dependent and transient impedance of grounding systems: Comparison between simulation and measurement," in *Lightning & Mountains* Chamonix, France, 1997.

[3] L. Grcev and F. Dawalibi, "An electromagnetic model for transients in grounding systems," *IEEE Trans. Power Delivery*, vol. 5, pp. 1773–1781, Oct. 1990.

[4] R. Velasquez and D. Mukhedkar, "Analytical modeling of grounding electrodes transient behavior," *IEEE Trans. Power Apparat. Syst.*, vol. PAS-103, pp. 1314–1322, June 1984.

[5] C. Mazzetti and G. Veca, "Impulse behavior of grounding electrodes," *IEEE Trans. Power Apparat. Syst.*, vol. PAS-102, pp. 3148–3156, Sept. 1983.

[6] A. P. Meliopoulos and M. G. Moharam, "Transient analysis of grounding systems," *IEEE Trans. Power Apparat. Syst.*, vol. PAS-102, pp. 389–397, Feb. 1983.

[7] S. Cattaneo, A. Geri, F. Mocci, and G. Veca, "Transient behavior of grounding systems simulation: Remarks on the EMTP's and special code's use," in *Proc. 21st EMTP Users Group Meeting*, Kolympari Crete, Greece, June 5–7, 1992.

[8] N. D. Hatziargyriou and M. Lorentzou, "Grounding systems design using EMTP," in *Proc. 23rd European EMTP Users Group Meeting*, Barcelona, Spain, November 9–11, 1997.

[9] M. Lorentzou and N. Hatziargyriou, "Modeling of long grounding conductors using emtp," in *Proc. Int. Conf. Power Syst. Transients*, Budapest, Hungary, June 20–24, 1999.

[10] R. G. Olsen and M. C. Willis, "A comparison of exact and quasistatic methods for evaluating grounding systems at high frequencies," *IEEE Trans. Power Delivery*, vol. 11, pp. 1071–1081, Apr. 1996.

[11] F. Menter, "Accurate modeling of conductors imbedded in earth with frequency dependent distributed parameter lines," in *Proc. 1st EMTP User Group Meeting*, 1992.
[12] ——, "EMTP based model for grounding system analysis," *IEEE Trans. Power Delivery*, vol. 9, pp. 1838–1849, Oct. 1994.
[13] J. Marti, "Accurate modeling of frequency dependent transmission lines in electromagnetic transient simulations," *IEEE Trans. Power Apparat. Syst.*, vol. PAS-101, pp. 135–147, Jan. 1982.
[14] S. Devgan and E. R. Whitehead, "Analytical models for distributed grounding systems," *IEEE Trans. Power Apparat. Syst.*, pt. III, vol. PAS-92, pp. 1763–1770, Sept./Oct. 1973.
[15] M. A. Uman, *The Lightning Discharge*. New York: Academic Press, 1987.
[16] A. C. Liew and M. Darveniza, "Dynamic model of impulse characteristics of concentrated earths," *Proc. Inst. Elect. Eng.*, vol. 121, no. 2, Feb. 1974.
[17] E. E. Oettle, "A new general estimation curve for predicting the impulse impedance of concentrated earth electrodes," in *Proc. IEEE/Power Eng. Soc. 1987 Winter Meeting*, Paper 87 WM 567-1 PWRD.
[18] S. Sekioka, H. Hayashida, T. Hara, and A. Ametani, "Measurements of grounding resistances for high impulse currents," *Proc. Inst. Elect. Eng. Generation and Distribution*, vol. 145, no. 6, Nov. 1998.

M. I. Lorentzou was born in 1971. She received the Ph.D. degree from the electrical and computer engineering department at National Technical University of Athens (NTUA), Greece, in 2001. Her research interests include the transient behavior of grounding systems, lightning protection of wind turbines, and calculation of power system transients.

Dr. Lorentzou is a member of the Technical Chamber of Greece.

N. D. Hatziargyriou (SM'90) received the diploma in electrical and mechanical engineering from National Technical University of Athens (NTUA), and the M.Sc. and Ph.D. degrees from University of Manchester Institute of Technology, U.K.

Currently, he is Professor at Power Division of the Electrical Engineering Department of NTUA. His research interests include power system transients, switching transients, dynamic security, and renewable energy sources.

He is senior member of IEEE and member of CIGRE SC 38 and of Technical Chamber of Greece.

B. C. Papadias (M'69–SM'73–F'97–LF'01) received the electrical engineering and Doctor of Engineering degree from National Technical University of Athens (NTUA), and the M.Sc. and Ph.D. degrees in electrical engineering from Rensselaer Polytechnic Institute, Troy, NY.

Currently, he is Professor of Electrical Energy Systems at NTUA. His research interests include dynamic analysis of power systems, interruption of small inductive currents, transient stability, switching transients, and renewable energy sources.

He is a Life Fellow member of IEEE and currently serves as Chairman of the European IEEE Chapter Co-ordinating Committee, member of CIGRE Administrative Council, and member of Technical Chamber of Greece.